GLOBAL CARDIOLOGY SCIENCE & PRACTICE
A Qatar Foundation Academic Journal

OPEN ACCESS

Research article

# Right ventricular mechanics in hypertrophic cardiomyopathy using feature tracking

Hala Mahfouz Badran[1,*], Mahmood Soliman[1], Hesham Hassan[1], Raed Abdelfatah[1], Haythem Saadan[1], Magdi Yacoub[2,3]

[1]Cardiology Department, Menoufiya University, Egypt
[2]Imperial College, London, UK
[3]Qatar Cardiovascular Research Center, Doha, Qatar
*Email: halamahfouz_1000@yahoo.com

## ABSTRACT

**Objectives:** Right ventricular (RV) mechanics in hypertrophic cardiomyopathy (HCM) are poorly understood. We investigate global and regional deformation of the RV in HCM and its relationship to LV phenotype, using 2D strain vector velocity imaging (VVI).

**Methods:** 100 HCM patients (42% females, 41 ± 19 years) and 30 control patients were studied using VVI. Longitudinal peak systolic strain ($\epsilon_{sys}$), strain rate (SR), time to peak ($\epsilon$) (TTP), displacement of RV free wall (RVFW) and septal wall were analyzed. Similar parameters were quantified in LV septal, lateral, anterior and inferior segments. Intra-V-delay was defined as SD of TTP. Inter-V-delay was estimated from TTP difference between the most delayed LV segment & RVFW.

**Results:** $\epsilon_{sys}$ and SR of both RV & LV, showed loss of base to apex gradient and significant decline in HCM ($p < 0.001$). Deformation variables estimated from RVFW were strongly correlated with each other ($r = 0.93$, $p < 0.0001$). Both were directly related to LV $\epsilon_{sys}$, $SR_{sys}$, $SR_e$, ejection fraction (EF)%, RVFW displacement ($P < 0.001$) and inversely related to age, positive family history ($p < 0.004$, 0.005), RV wall thickness, maximum wall thickness (MWT), intra-V-delay, LA volume ($P < 0.0001$), LVOT gradient ($p < 0.02$, 0.005) respectively. ROC curves were constructed to explore the cut-off point that discriminates RV dysfunction. Global and RVFW $\epsilon_{sys}$: −19.5% shows 77, 70% sensitivity & 97% specificity, $SR_{sys}$: $-1.3s^{-1}$ shows 82, 70% sensitivity & 30% specificity. Multivariate analyses revealed that RVFW displacement ($\beta = -0.9$, $p < 0.0001$) and global LV $SR_{sys}$ ($\beta = 5.9$, $p < 0.0001$) are independent predictors of global RV deformation.

**Conclusions:** Impairment of RV deformation is evident in HCM using feature tracking. It is independently influenced by LV mechanics and correlated to the severity of LV phenotype. RVFW deformation analysis and global RV assessment are comparable.

*Keywords:* right ventricular deformation, hypertrophic cardiomyopathy, feature tracking

http://dx.doi.org/10.5339/gcsp.2013.25

Submitted: 03 March 2013
Accepted: 04 June 2013
© 2013 Badran, Soliman, Hassan, Abdelfatah, Saadan, Yacoub, licensee Bloomsbury Qatar Foundation Journals. This is an open access article distributed under the terms of the Creative Commons Attribution license CC BY 3.0, which permits unrestricted use, distribution and reproduction in any medium, provided the original work is properly cited.

QSCIENCE.com
Member of Qatar Foundation

Cite this article as: Badran HM, Soliman M, Hassan H, Abdelfatah R, Saadan H, Yacoub M. Right ventricular mechanics in hypertrophic cardiomyopathy using feature tracking, *Global Cardiology Science and Practice* 2013:25 http://dx.doi.org/10.5339/gcsp.2013.25

## INTRODUCTION

Right ventricular (RV) chamber is often involved in left ventricular (LV) pathologies as a consequence of a direct injury extension, afterload changes, or ventricular interdependence, which is mainly due to the close anatomic association between the two ventricles.[1–3]

Over the last 50 years, awareness regarding the characterization of hypertrophic cardiomyopathy (HCM) has evolved dramatically in terms of phenotypic expression, pathophysiology, and clinical course.[4–6] It is reasonable that the right ventricle may participate in the disease because of an extension of myopathic processes and/or because right and left ventricles share structurally hypertrophied interventricular septum.

At times, termed 'the forgotten ventricle', the right ventricle can prove difficult to accurately and reproducibly assess, as a result of its shape and volume dependency.[3,7] Previous studies have shown an increased RV wall thickness and RV diastolic dysfunction in a large proportion of patients affected by HCM by using magnetic resonance imaging, 2D echocardiography, and biplane RV angiography.[8–10] However, few data are presently available about RV regional and global modifications in this pathology.[11,12]

Recent developments have improved cardiac function quantification and it seems that both magnitude and temporal sequence of tissue deformation can provide additional information in different cardiac diseases.[13]

On this basis, the aim of the present study was to analyze the assorted involvement of RV myocardial function in HCM using 2D strain vector velocity imaging (VVI).

This is a novel feature tracking technique that uses myocardial speckle to assess cardiac mechanics. It uses an algorithm that automatically tracks motion of the tissue-cavity border and motion of reference points, showing tissue displacement, direction, and velocity. It also provides accurate information about segmental myocardial deformation during the cardiac cycle and has the additional advantage of assessing systolic and diastolic function of both ventricles independent of Doppler interrogation angle.[14,15]

## PATIENTS AND METHODS

### Study population

#### HCM group

Between January 2011 and December 2011, we prospectively included 100 HCM patients (age range: 8–77 years), who were referred to our echocardiographic laboratories for risk stratification. They were examined in a single centre (Yacoub Research Unite, Menoufiya University, Egypt). Patients were enrolled in the study after their informed consent, and approval of the Ethics Committee of Menoufiya University Hospitals was obtained.

The diagnosis of HCM was based on conventional echocardiographic demonstration of a non-dilated, hypertrophic LV ($\geq$ 15 mm) in the absence of other cardiac or systemic diseases capable of producing the magnitude of hypertrophy evident.[2] Exclusion criteria were diabetes mellitus, arterial hypertension, and evidence of coronary artery disease, atrial fibrillation, lung disease, and inadequate echocardiograms.

#### Control group

We studied 33 age and sex-matched healthy subjects without detectable cardiovascular risk factor or receiving any medication. Volunteer controls were all selected from departments of pediatric and adult cardiology among subjects investigated for either sport or work eligibility.

### Conventional Echocardiography

Echocardiographic exams were performed with all subjects positioned in the left lateral decubitus, by the same operator (HM) in the parasternal long, short-axis, apical 2- & 4-chamber views using standard transducer positions. Esaote Mylab Gold 30 ultrasound system (Esaote S.p.A, Florence, Italy) equipped with a multi-frequency 2.5–3.5 MHz phased-array transducer was utilized.[16,17] RV end diastolic diameter and wall thickness, LV end diastolic (LVEDD), end systolic diameter (LVESD), septum (SPT), posterior wall thickness (PWT), ejection fraction (EF%) and left atrial (LA) diameter & volume were all measured in accordance with the recommendations of the American Society of Echocardiography.[18] The magnitude and extent of hypertrophy in both ventricles were assessed in all views. Color flow

mapping and continuous-wave Doppler was used to define resting LVOT, mid cavity & RV obstruction, and to estimate pulmonary artery pressure (PAP) from tricuspid regurgitation velocity (Bernoulli equation). Peak early (E) and late (A) transmitral ($E_m$ & $A_m$) and trantricuspid ($E_t$ & $A_t$) filling velocities were measured from mitral and tricuspid inflow velocities. Peak systolic ($S_a$), early diastolic ($E_a$) and atrial diastolic ($A_a$) velocity and isovolumetric relaxation time (IRT) were obtained by placing a tissue Doppler myocardial imaging (DMI) sample volume at the RVFW and lateral mitral annulus in the apical 4-chamber view. The $E_m/E_{am}$ and $E_t/E_{at}$ ratio were calculated.

### Deformation imaging

Border tracking of the left ventricle (LV) and right ventricle (RV) was manually traced in the recorded clips of apical 4C & 2C views, with good quality ECG signal and a frame rate between 40–70 fps. They were then stored for offline analysis using XStrain™ software. VVI is dedicated software that derives longitudinal myocardial velocity, strain (ϵ), strain rate (SR) and displacement from digitized 2D video clips. The endocardial border is automatically drawn at end diastole using a point-and-click approach. For RV it was tracked from the septal side of the tricuspid annulus to RV free wall side and for the LV from septal to lateral side of mitral annulus in apical 4C and from anterior to inferior side in the apical 2C. Velocity, ϵ, and SR, displacement graphics were automatically obtained[17] (Figure 1,2).

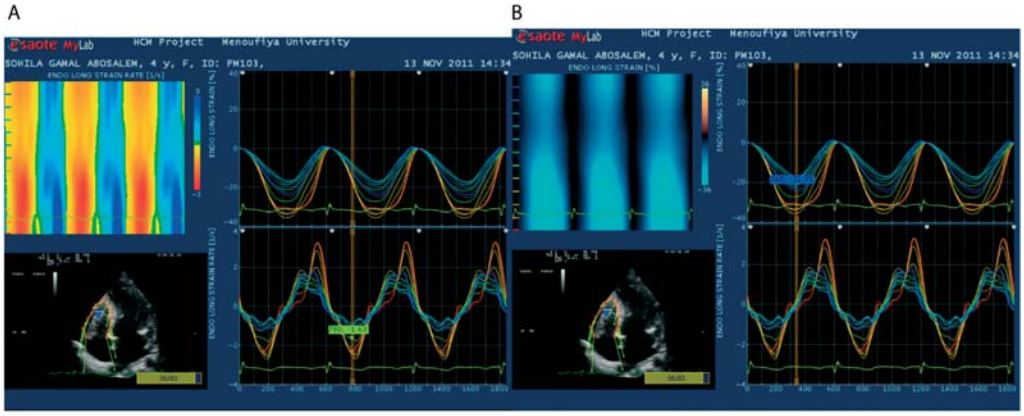


**Figure 1. RV deformation analysis in apical 4C view. The vectors show the direction of motion of any point selected on bottom left, on upper left color scale analysis of systolic strain, on the right side curves of Strain ($\epsilon_{sys}$) and SR of all selected points. (A)The mean $\epsilon_{sys}$ is −22.9%, (B)$SR_{sys}$ is $-1.63s^{-1}$.**

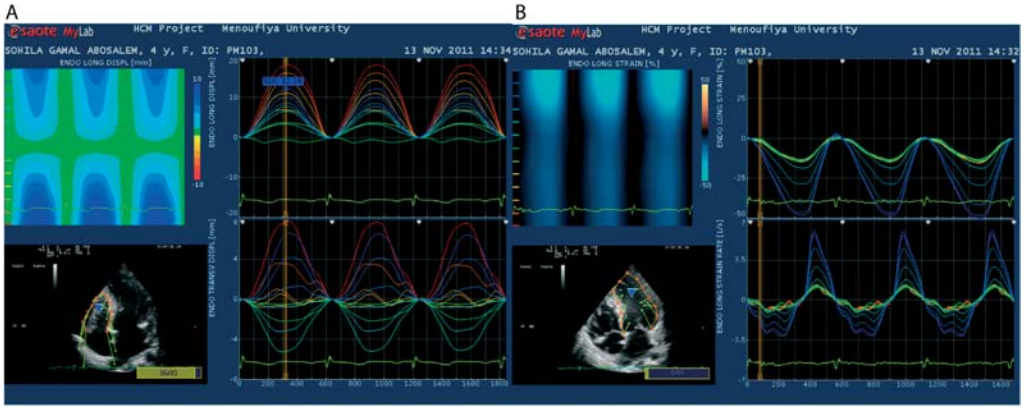


**Figure 2. LV deformation in apical 4C of same HCM patient: (A) on the right side curves of Strain ($\epsilon_{sys}$) and SR of LV selected points. (B) RV longitudinal displacement (upper right) and transverse displacement (lower right).**

### Analysis of RV and LV deformation

Longitudinal $\epsilon_{sys}$, systolic SR ($SR_{sys}$), early diastolic ($SR_e$), atrial diastolic ($SR_a$) and post-systolic shortening (PSS) in the basal, mid and apical segments of RVFW and septum were measured. Global RV deformation was calculated from RVFW and septal segments. For LV deformation the same

parameters were measured for basal, mid and apical segments of septal, lateral, anterior and inferior wall. To reduce random noise, each sample was obtained by averaging three consecutive heart cycles.

To estimate mechanical dyssynchrony, the index of myocardial systolic activation was calculated from regional strain curves for each ventricular segment, as a function of time from the beginning of Q-wave of ECG to the peak longitudinal systolic strain (TTP). RV and LV electromechanical delay was measured as the difference between TTP (d-TTP) in 6 RV and 12 LV segments respectively (difference between the longest and shortest times[19,20]).

Intra-V dyssynchrony was defined as the standard deviation of the averaged time-to-peak-strain (TTP-SD). Inter-V dyssynchrony was estimated from TTP difference between the most delayed LV segment and RVFW.[21,22]

### Inter and Intra-observer variability

Two independent observers performed two separate quantitative strain and strain rate analyses of RV and LV images, blindly, in 28 participants. Interobserver and Intraobserver agreement for $\epsilon_{sys}$ data was: (for LV $\epsilon_{sys}$, R = 0.87 and 0.94, for RV $\epsilon_{sys}$, R = 0.87 and 89, for TTP, R = 0.90 and 0.98, respectively) and $SR_{sys}$ (interobserver R = 0.86, intraobserver R = 90). Both inter and intraobserver agreement were lower for diastolic SR (For $SR_e$: R = 0.82 and 0.87, respectively) and (For $SR_a$: R = 0.82 and 0.84, respectively).

### Statistical analyses

Data were presented as numbers (%) or mean ± SD. The distribution of qualitative variables was analyzed by chi-square test or Fisher's exact test. Means of patients' groups were compared by the unpaired Student test. Quantitative variables were correlated by the use of Pearson's correlation coefficient "r". All tests were 2-tailed and p value $\leq 0.05$ was considered statistically significant. To identify significant independent predictors of global RV strain, variables that were statistically significant in univariate analysis were introduced in a multivariate regression model; the overall fitness of the model was evaluated with the calculation of the coefficient R ± SE and its overall statistical significance was tested by ANOVA. Receiver operating characteristic (ROC) curve analysis was performed to select optimal cut-off values of clinical and echo measurements. The analysis was performed by the statistical software package IBM SPSS Statistics version 19.

## RESULTS

### Clinical characteristics of the study population

Demographic and clinical characteristics of studied groups are outlined in Table 1. No differences were observed between HCM and control group in age, gender, BSA, heart rate or blood pressure. From 100 HCM patients (42% females), 71% were symptomatic (~ 63% are NYHA class II, 35% class III, 2% class IV) and 8 (11%) had a history of syncope. 37 were familial-type (based on prospective evaluation of relatives), 16% had positive family history of premature sudden death, 79% had asymmetric septal hypertrophy, 18% had concentric LVH and 3% had apical HCM. 22 patients had extreme LVH (MWT ≥ 30 mm), 23% had LVOTO ≥ 30 mmHg, 21% had RV apical trabecular hypertrophy, 4% had RV obstruction at mid & apical region, 49% had RV diameter > 30 mm, 3% had severe tricuspid regurgitation and 20% had PAP > 30 mmHg (range: 30–82 mmHg).

### Conventional echocardiographic analysis

There was no significant difference among the two groups in LV EF%, RV diameter, $E_m$ inflow velocity.

LA dimension, volume, SPT and LVPW thickness, LVM, LVMI and LVOT gradient, $A_m$ inflow velocity, mitral IRT, tricuspid IRT, RVFW thickness were significantly greater, whereas LVESD, LVEDD, $E_m/A_m$ were significantly reduced in HCM group ($p < 0.001$).

LV and RV end diastolic pressure as estimated by $E_m/E_{am}$ and $E_t/E_{at}$ ratios were significantly elevated in comparison to the control group ($P < 0.001$, $< 0.01$) respectively.

### LV deformation analysis (Table 2)

In HCM, 2D strain analysis detected lower global and regional peak myocardial $\epsilon_{sys}$, $SR_{sys}$ and $SR_e$ ($P < .001$) at the level of all analyzed segments in comparison to control

**Table 1. Clinical and conventional echocardiographic criteria.**

| | HCM (n = 100) | Control (n = 30) | P value* |
|---|---|---|---|
| Age (years) | 41.1 ± 19.1 | 38.3 ± 8.6 | Ns. |
| Female sex | 42 (42%) | 7 (23%) | Ns. |
| BSA | 1.8 ± 0.36 | 1.85 ± 0.16 | Ns. |
| Heart rate | 74.6 ± 28.7 | 75.1 ± 9.9 | Ns. |
| SBP (mmHg) | 130 ± 18.1 | 120 ± 9 | Ns. |
| DBP (mmHg) | 84.2 ± 12.8 | 81 ± 6.5 | Ns. |
| LA diameter (mm) | 37.4 ± 9.1 | 30.9 ± 4.6 | 0.001 |
| LA volume (ml) | 63.8 ± 34.9 | 21.7 ± 8.7 | 0.001 |
| AoSD | 27.41 + 5.2 | 32.4 ± 3.61 | 0.001 |
| SAM (%) | 20 (20%) | | |
| LVOTO | 23 (23%) | | |
| **Mitral regurge:** | 2 (2%) | 30 (100%) | Ns. |
| no | 35 (35%) | | |
| Trivial | 35 (35%) | | |
| Mild | 21 (21%) | | |
| Moderate | 7 (7%) | | |
| Severe | | | |
| LVESD (mm) | 21.8 ± 6.5 | 33.2 ± 5.7 | 0.001 |
| LVEDD (mm) | 36.1 ± 7.8 | 45.8 ± 6.7 | 0.001 |
| FS% | 40.6 ± 10 | 39.6 ± 8.6 | Ns. |
| EF% | 71.2 ± 11.5 | 64.4 ± 10.4 | Ns. |
| MWT (mm) | 25.9 ± 7.1 | 9.9 ± 2.2 | 0.001 |
| SPT (mm) | 24.6 ± 6.9 | 9.9 ± 2.2 | 0.001 |
| LVPW (mm) | 14.4 ± 3.9 | 9.6 ± 2.1 | 0.001 |
| SPW ratio | 1.81 ± 0.67 | 1 ± 0.21 | 0.001 |
| LVM (gm) | 401 ± 188 | 197 ± 67 | 0.001 |
| LVMI (gm/m$^2$) | 222 ± 94 | 112.4 ± 32.6 | 0.001 |
| LVOTO (mmHg) | 29 ± 44.1 | 2.96 ± 1.2 | 0.002 |
| Mitral E (m/sec) | 0.86 ± 3.5 | 0.76 ± 0.13 | Ns. |
| Mitral A (m/sec) | 1.27 ± 5.8 | 0.52 ± 0.13 | 0.001 |
| Mitral E/A | 0.68 ± 0.62 | 1.2 ± 0.13 | 0.001 |
| DT (ms) | 192 ± 70.5 | 140 ± 56 | Ns. |
| PAP (mmHg) | 28.9 ± 16.3 | 12.3 ± 2.2 | 0.01 |
| Mitral IRT | 93 ± 12.3 | 69.5 ± 7 | 0.001 |
| $E_m/E_{am}$ | 12 ± 7.7 | 6.2 ± 3.8 | 0.001 |
| $E_t/E_{at}$ | 10.5 ± 4.4 | 7.6 ± 3.2 | 0.01 |

* Chi-Square test or Student's test. Ns.: non-significant, BSA: body surface area; SBP: systolic blood pressure; DBP: diastolic blood pressure, LVH: left ventricular hypertrophy, AoSD: aortic systolic diameter, SAM: systolic anterior motion, LVESD: left ventricular end-systolic diameter, LVEDD: left ventricular end-diastolic diameter, FS: fractional shortening, EF: ejection fraction, MWT: maximal wall thickness, LVPW: posterior wall thickness, SPT: septal thickness, LVM: left ventricular mass, LVMI: left ventricular mass index, LVOT: left ventricular outflow tract, DT: deceleration time, PAP: pulmonary artery pressure.

Despite the significant difference of $SR_a$ at some segmental levels, the global atrial diastolic SR did not differ from the control. PSS within LV segments was exceedingly prevalent in HCM (57% vs 0% in control) and depicted in more than one segment (1.22 ± 1.56). Similarly, electromechanical delay was considerably prolonged in all LV segments, compared with its corresponding segments in healthy individuals ($P < .001$). Intra-V dyssynchrony (TTP-SD) was significantly greater in HCM (63.9 ± 37.2) compared with control (29.2 ± 16.4) $p < 0.0001$.

## Regional and global RV deformation (Table 3)

Both longitudinal $\epsilon_{sys}$ and SR values showed a base-to-apex gradient in the control group. RV deformation parameters showed a loss of this gradient and significant decline in HCM group. The averaged RVFW segments $\epsilon_{sys}$(−14.7 ± 10.3 vs −25.4 ± 2.9%) $SR_{sys}$(−1.12 ± 0.74 vs −1.6 ± 0.53$s^{-1}$) and $SR_e$ (0.95 ± 0.71 vs 1.69 ± 0.42 $s^{-1}$) were significantly reduced in the HCM group compared with control group ($p < 0.001$ for each). These findings were also apparent in global RV deformation and gave similar significance ($p < 0.001$) with the exception of atrial diastolic SR ($P =$ Ns.).

For electromechanical delay between RV segments, controls showed homogeneous systolic activation of the ventricular walls. Conversely, the HCM group, despite the absence of intraventricular conduction defects by surface ECG, showed significant prolongation of TTP of all RV segments ($p < 0.001$). Inter−V dyssynchrony was also verified and showed significant increase in HCM (68.2 ± 113 vs 24 ± 16 ms, $p < 0.001$) compared with control group. PSS in RVFW was depicted in one or more segments in 30% of studied HCM series.

**Table 2. Left ventricular deformation parameters.**

| | HCM (n = 100) | Control (n = 30) | P value* |
|---|---|---|---|
| $\epsilon_{sys}$ % septum | −11.7 ± 6.5 | −19.6 ± 1.9 | 0.001 |
| $\epsilon_{sys}$% lateral | −12.4 ± 7.4 | −19.95 ± 2.2 | 0.001 |
| $\epsilon_{sys}$ % anterior | −12.5 ± 9 | −19.6 ± 2 | 0.001 |
| $\epsilon_{sys}$% inferior | −11.5 ± 7.2 | −19.8 ± 2.3 | 0.001 |
| **$\epsilon_{sys}$% global LV** | **− 8.57 ± 6.8** | **− 20.4 ± 1.1** | **0.001** |
| PSS (%) | 57 (57%) | 0 | |
| PSS (no. of seg) | 1.22 ± 1.56 | 0 | |
| Mean TTP (ms) | 407.1 ± 112 | 350.5 ± 33.1 | 0.001 |
| LV d-TTP | 189 ± 70 | 92 ± 21 | 0.001 |
| **TTP-SD** | **63.9 ± 37.2** | **29.2 ± 16.4** | **0.001** |
| $SR_{sys}$ $s^{-1}$ septum | −0.74 ± 0.45 | −1.23 ± 0.35 | 0.001 |
| $SR_{sys}$ $s^{-1}$ lateral | −0.79 ± 0.47 | −1.32 ± 0.19 | 0.001 |
| $SR_{sys}$ $s^{-1}$ anterior | −0.76 ± 0.37 | −1.24 ± 0.33 | 0.001 |
| $SR_{sys}$ $s^{-1}$ inferior | −0.78 ± 0.40 | −1.34 ± 0.20 | 0.001 |
| **$SR_{sys}$ $s^{-1}$global LV** | **− 0.78 ± 0.36** | **− 1.3 ± 0.21** | **0.001** |
| $SR_e$ $s^{-1}$ septum | 0.7 ± 0.48 | 1.49 ± 0.47 | 0.001 |
| $SR_e$ $s^{-1}$ lateral | 0.80 ± 0.56 | 1.61 ± 0.32 | 0.001 |
| $SR_e$ $s^{-1}$ anterior | 0.85 ± 0.56 | 1.52 ± 0.46 | 0.001 |
| $SR_e$ $s^{-1}$ inferior | 0.89 ± 0.47 | 1.64 ± 0.36 | 0.001 |
| **$SR_e$ $s^{-1}$ global LV** | **0.81 ± 0.54** | **1.57 ± 0.3** | **0.001** |
| $SR_a$ $s^{-1}$ septum | 0.45 ± 0.28 | 0.62 ± 0.12 | 0.002 |
| $SR_a$ $s^{-1}$ lateral | 0.45 ± 0.31 | 0.61 ± 0.15 | 0.009 |
| $SR_a$ $s^{-1}$ anterior | 0.46 ± 0.32 | 0.61 ± 0.13 | 0.012 |
| $SR_a$ $s^{-1}$ inferior | 0.98 ± 4.68 | 0.63 ± 0.13 | Ns. |
| **$SR_a$ $s^{-1}$ global LV** | **0.59 ± 1.26** | **0.62 ± 0.11** | **Ns.** |

* Student's test. Ns.: non-significant, **$\epsilon_{sys}$**: peak systolic strain, LV: left ventricle, TTP: time to peak strain, TTP-SD: standard deviation of time to peak strain, $SR_{sys}$: peak systolic strain rate, $SR_e$: early diastolic strain rate, $SR_a$: atrial diastolic strain rate.

### Univariate relations of RV 2D-strain indexes (Table 4, Figures 3&4)

In HCM, the deformation variables estimated by RVFW were concordant with those derived by RV global assessment. RVFW and RV global strain strongly correlated with each other ($r = 0.93$, $p < 0.0001$). Both were directly related to LV $\epsilon_{sys}$, $SR_{sys}$ and $SR_e$, EF%, RVFW displacement ($p < 0.001$) and inversely related to age, positive family history ($p < 0.004$, 0.005), RV wall thickness, MWT ($p < 0.0001$), LV dyssynchrony (TTP-SD, $p < 0.0001$), LA volume ($p < 0.0001$), LVOT gradient ($p < 0.02$, 0.005) LVESD ($p < 0.001$, 0.002) and EDD ($p < 0.002$, 0.03) respectively. Only global RV strain was negatively correlated to LVM, LVMI ($p < 0.01$, 0.006) respectively. Conversely, RV regional and global strain were not linked to NYHA functional class, $E_m/E_{am}$ or $E_t/E_{at}$ ratios, PAP or PSS in this HCM series.

To explore the cutoff point that discriminate RV dysfunction we constructed ROC curves for RV $\epsilon_{sys}$, $SR_{sys}$, $SR_e$ and $SR_a$ in HCM (Figure 5). For global and RVFW $\epsilon_{sys}$ − 19.5% shows 77, 70% sensitivity and 97% specificity respectively, AUC: 0.862 [CI: 0.798–0.923, P < .0001]. Global and RVFW SR $_{sys}$ −1.3% shows 82, 70 % sensitivity and 30% specificity with AUC 0.769 [CI: 0.686–0.853, P < .0001]. For diastolic function; global and RVFW $SR_e$, cutoff value 1.4 shows 91, 82% sensitivity and 92, 83% specificity respectively. In addition, Global $SR_a$ 0.78 shows 81% sensitivity, 40% specificity, while RVFW $SR_a$: 1.02 has 80% sensitivity& 40% specificity respectively. It seems that SR parameters were less specific than $\epsilon_{sys}$ in differentiation of RV dysfunction in HCM.

### Multivariate analysis

Stepwise, forward, multiple linear regression analyses were performed in the overall population to weigh the independent associations between global RV myocardial strain and LV phenotype. With this model, after adjusting for potential determinants, only global LV $SR_{sys}$ (B coefficient = 5.9; IC at 95%: 3.06–8.75) and mean RVFW displacement (B coefficient −0.9; CI at 95%: −1.09 – −0.71) are independent predictors for global RV strain; $p < 0.0001$. The model significantly explained the outcome variable (global RV strain), R ± SE = 0.922 ± 2.96; $p < 0.0001$.

## DISCUSSION

Current research in clinical cardiac mechanics is moving from LV short axis and ejection fraction to long-axis function, and from global to regional deformation abnormalities in different myocardial diseases. Measurement of longitudinal strain (rate) in the RV can be regarded as a reliable measure

**Table 3. Right ventricular regional and global deformation.**

| | HCM (n = 100) | Control (n = 30) | P value* |
|---|---|---|---|
| RV diameter (mm) | 31 ± 6.35 | 30.8 ± 5.87 | Ns. |
| RV thickness (mm) | 11.5 ± 6.35 | 6.3 ± 2.5 | 0.001 |
| Tricuspid IRT | 80.2 ± 12 | 59.4 ± 8.3 | 0.001 |
| TASV cm/s | 6.18 ± 3.75 | 9.69 ± 2.31 | 0.001 |
| TAEV cm/s | 4.63 ± 2.95 | 8.14 ± 2.23 | 0.001 |
| TAAV cm/s | 4.42 ± 2.72 | 5.99 ± 2.2 | 0.006 |
| $\epsilon_{sys}$ (%) basal RVFW | −19.0 ± 2.1 | −22.1 ± 5.02 | 0.04 |
| $\epsilon_{sys}$ (%) mid RVFW | −14.8 ± 12.4 | −26.7 ± 3.7 | 0.001 |
| $\epsilon_{sys}$ (%) apical RVFW | −7.3 ± 9.28 | −27.5 ± 4.2 | 0.001 |
| **$\epsilon_{sys}$ (%) mean RVFW** | **−14.7 ± 10.3** | **−25.4 ± 2.9** | **0.001** |
| **$\epsilon_{sys}$ (%) global RV** | **−13.2 ± 7.3** | **−22 ± 1.73** | **0.001** |
| PSS (%) | 35 (35%) | 0 | |
| PSS (no. of seg) | 0.51 ± 0.79 | 0 | |
| TTP basal RVFW **(ms)** | 394 ± 139 | 380 ± 33 | Ns. |
| TTP mid RVFW **(ms)** | 400 ± 139 | 332 ± 31 | 0.001 |
| TTP apical RVFW **(ms)** | 410 ± 160 | 376 ± 31 | 0.001 |
| RVFW mean TTP **(ms)** | 401 ± 137 | 372 ± 30 | Ns. |
| **TTP global RV (ms)** | **395 ± 107** | **324 ± 25** | **0.001** |
| **Inter-V dyssyn (ms)** | **68.2 ± 113** | **24.2 ± 16.3** | **0.001** |
| $SR_{sys}$ $s^{-1}$ basal RVFW | −1.1 ± 1.1 | −1.39 ± 0.66 | Ns. |
| $SR_{sys}$ $s^{-1}$ mid RVFW | −1.09 ± 1.14 | −1.71 ± 0.56 | 0.005 |
| $SR_{sys}$ $s^{-1}$ apical l RVFW | −0.56 ± 0.63 | −1.97 ± 0.49 | 0.001 |
| **$SR_{sys}$ $s^{-1}$ Mean RVFW** | **−1.12 ± 0.74** | **−1.69 ± 0.53** | **0.001** |
| **$SR_{sys}$ $s^{-1}$ global RV** | **−0.93 ± 0.46** | **−1.46 ± 0.31** | **0.001** |
| $SR_e$ $s^{-1}$ basal RVFW | 1.43 ± 1.17 | 1.74 ± 0.57 | 0.002 |
| $SR_e$ $s^{-1}$ mid RVFW | 0.91 ± 0.9 | 1.62 ± 0.42 | 0.001 |
| $SR_e$ $s^{-1}$ apical RVFW | 0.52 ± 0.53 | 2.32 ± 0.41 | 0.001 |
| **$SR_e$ $s^{-1}$ mean RVFW** | **0.95 ± 0.71** | **1.69 ± 0.42** | **0.001** |
| **$SR_e$ $s^{-1}$ global RV** | **0.83 ± 0.48** | **1.59 ± 0.32** | **0.001** |
| $SR_a$ $s^{-1}$ basal RVFW | 1.06 ± 0.91 | 1.33 ± 0.44 | Ns. |
| $SR_a$ $s^{-1}$ mid RVFW | 1.59 ± 3.68 | 1.36 ± 0.29 | Ns. |
| $SR_a$ $s^{-1}$ apical RVFW | 0.39 ± 0.33 | 1.93 ± 0.37 | 0.001 |
| **$SR_a$ $s^{-1}$ mean RVFW** | **1.01 ± 2.95** | **1.11 ± 0.32** | **Ns.** |
| **$SR_a$ $s^{-1}$ global RV** | **0.74 ± 1.51** | **0.86 ± 0.16** | **Ns.** |
| Basal RVFW displac. | 10.2 ± 7.5 | 10.9 ± 3.27 | Ns. |
| Mid RVFW displac. | 4.03 ± 4.4 | 11.05 ± 2.59 | 0.001 |
| Apical RVFW displac. | 0.95 ± 2.54 | 12.4 ± 3.29 | 0.001 |
| mean RVFW displac. | 5.06 ± 3.97 | 10.8 ± 2.73 | 0.001 |

* Student's test. Ns.: non-significant, RV: right ventricle, RVFW: RV free wall, TAPSV: tricuspid annular systolic velocity, TAPEV: tricuspid annular plane early diastolic velocity, TAPAV: tricuspid annular plane atrial diastolic velocity, dyssyn: dyssynchrony, $\epsilon_{sys}$: peak systolic strain, LV: left ventricle, TTP: time to peak strain, TTP-SD: standard deviation of time to peak strain, $SR_{sys}$: peak systolic strain rate, $SR_e$: early diastolic strain rate, $SR_a$: atrial diastolic strain rate, displac: displacement.

for (global) RV myocardial function and ejection fraction, even more than in the LV, since 80% of total stroke volume is generated by longitudinal shortening.[22]

This study with special focus on the RV provides new insights into mechanical alteration in the RV using feature tracking. Quantitative RV functional evaluation revealed a reduction in systolic and diastolic deformation, which is strongly correlated with LV phenotype in HCM. Global LV systolic strain rate and RVFW displacement was independent predictor to RV dysfunction. The most important finding of this study was that RVFW mechanics was closely related to global RV deformation and gave the same clinical correlates. The former might consequently be used as an alternative measure of RV pump function.

Previous experimental and clinical studies indicate that the septum is 'the lion of right ventricular function' and the fiber orientation and septal architecture & function is essential for RV ejection and suction for rapid filling.[23] However, in the present study, despite septal hypertrophy and dysfunction due to involvement by myopathic process, the RVFW still playing important role in overall RV performance as its abnormal deformation was not only contributor but also representative to global RV deformation. Both RVFW and global RV longitudinal deformation was firmly parallel and were directly related to LV systolic and diastolic function and inversely related to familial type, magnitude of hypertrophy, severity of obstruction and LV dyssynchrony.

## RV diastolic function

In concordance with previous studies, we ascertained significantly lower early diastolic myocardial velocity and $SR_e$ and increased $IRT_t$, $E_t/E_{at}$ that reflects elevated right ventricular end-diastolic

**Table 4. Correlation between global RV $\epsilon_{SYS}$% and RVFW $\epsilon_{SYS}$ and other clinical parameters.**

| global RV $\epsilon_{sys}$ | $\epsilon_{SYS}$ global LV | SR $_{SYS}$ global LV | $SR_e$ global LV | $SR_a$ global LV | RV diameter | RV thickness | MWT | LVOT gradient | Age | NYHA functional class | LV TTP-SD | LA volume |
|---|---|---|---|---|---|---|---|---|---|---|---|---|
| r = | 0.748 | 0.752 | 0.664 | − 0.071 | 0.053 | 0.373 | − 0.407 | 0.261 | − 0.336 | 0.123 | − 0.427 | − 0.351 |
| P | 0.0001 | 0.0001 | 0.0001 | Ns. | Ns. | 0.0001 | 0.0001 | 0.004 | 0.0001 | Ns. | 0.0001 | 0.0001 |
| RVFW $\epsilon_{sys}$ r = | 0.641 | 0.552 | 0.503 | − 0.039 | 0.091 | 0.319 | − 0.27 | 0.202 | − 0.332 | 0.109 | − 0.418 | − 0.229 |
| P | 0.0001 | 0.0001 | 0.0001 | Ns. | Ns. | 0.0001 | 0.002 | 0.025 | 0.0001 | Ns. | 0.0001 | 0.01 |
| **Global RV $\epsilon_{sys}$** | **EF%** | **LVM** | **LVMI** | **Et/Eta** | **PAP** | **DT** | **PSS LV** | **LVESD** | **LVEDD** | **RVFW displacement** | **RVFW $\epsilon_{sys}$** | **+ ve FH** |
| r = | 0.25 | − 0.229 | − 0.242 | 0.202 | 0.076 | − 0.065 | − 0.013 | − 0.352 | − 0.278 | 0.834 | 0.932 | − .27 |
| P | 0.005 | 0.01 | 0.006 | Ns. | Ns. | Ns. | Ns. | 0.0001 | 0.002 | 0.0001 | 0.0001 | 0.004 |
| RVFW $\epsilon_{sys}$ r = | 0.226 | 0.137 | 0.11 | 0.154 | 0.025 | − 0.03 | − 0.051 | − 0.277 | − 0.187 | 0.842 | 1 | − .24 |
| P | 0.011 | Ns. | Ns. | Ns. | Ns. | Ns. | Ns. | 0.002 | 0.036 | 0.0001 | | 0.005 |

RV: right ventricle, Ns.: non-significant, RVFW: RV free wall, $\epsilon_{sys}$: peak systolic strain, LV: left ventricle, $SR_{sys}$: peak systolic strain rate, $SR_e$: early diastolic strain rate, $SR_a$: atrial diastolic strain rate, MWT: maximal wall thickness, LVOT: LV outflow tract, TTP-SD: SD of time to peak, LA: left atrium, EF: ejection fraction, LVMI: LV mass index, Et/Eta: tricuspid early Doppler inflow/tricuspid annular velocity, PAP: pulmonary artery pressure, DT: deceleration time, PSS: post systolic strain, LVESD: LV end systolic diameter, LVEDD: LV end diastolic diameter, + ve FH: positive family history.

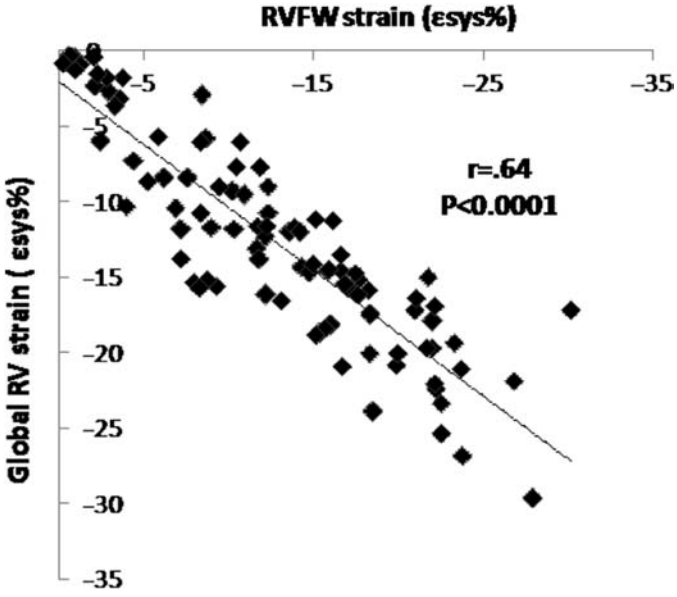


**Figure 3.** Direct relation between RV free wall longitudinal strain ($\epsilon_{sys}$) and RV global strain in the HCM group.

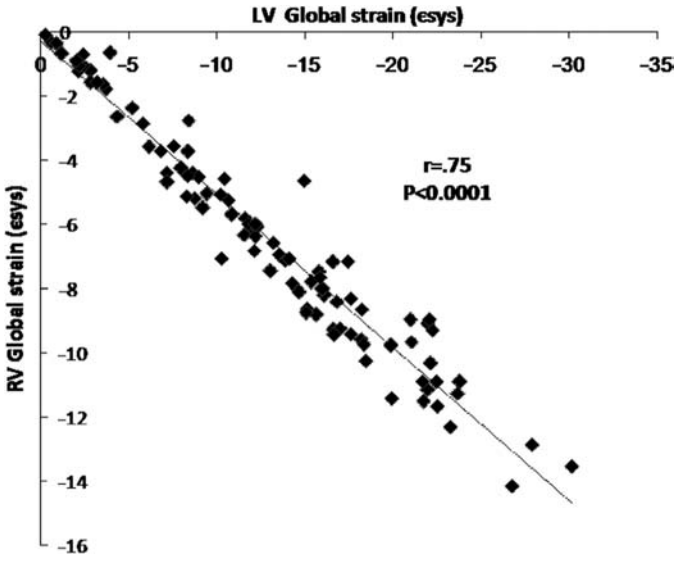


**Figure 4.** Direct relation between RV global strain ($\epsilon_{sys}$) and global LV strain ($\epsilon_{sys}$) in HCM group.

pressures (RVEDP) in comparison to the control, confirming a pattern of impaired RV filling. RV diastolic dysfunction was observed by Maeda et al.,[24] who described impaired RV isovolumic relaxation by biplane RV angiography, and by Suzuki et al.[25] who found lower early peak filling rate by magnetic resonance. Furthermore, in previous reports analyzing the RV Doppler inflow, Okamoto et al.[26] and Lazzaret et al.[27] described slow deceleration of rapid filling wave, increase in the lengthening of atrial contraction, and reduction of tricuspid E/A ratio. The present study verified RV myocardial diastolic dysfunction in HCM, since RV global $\epsilon_{sys}$ and regional 2D $SR_e$ and $SR_a$ peaks were significantly impaired, despite clinical evidence of RV failure is not exist.

## RV function using feature tracking

Integration of new evidence in basic science and evolutions in imaging technology must be matched with a new understanding of cardiac mechanics to provide insights into disease that can lead to new therapies.[17]

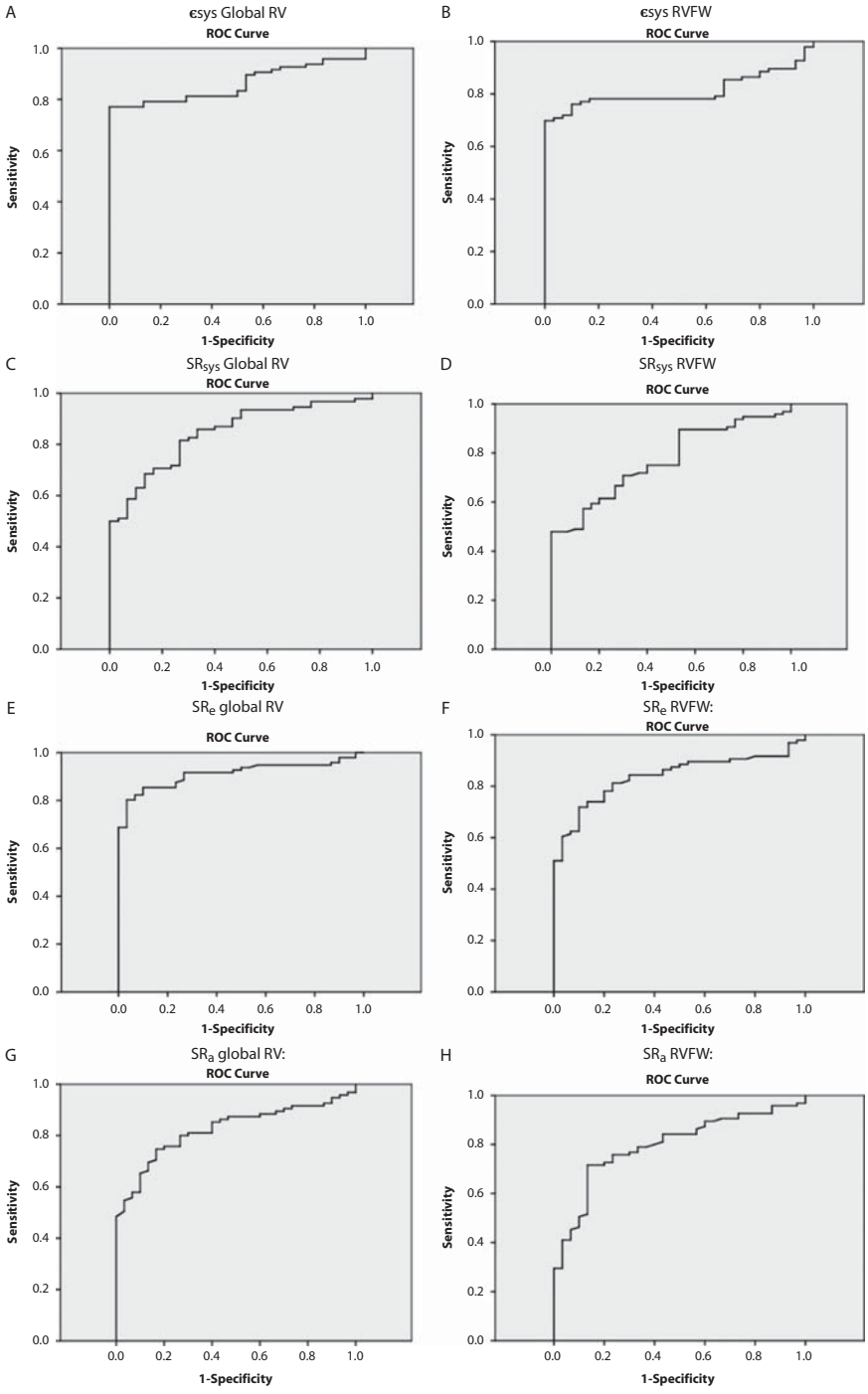


**Figure 5. ROC curve of global and RVFW deformation parameters has been plotted for differentiating HCM patients with RV dysfunction. (A) $\epsilon_{sys}$ global RV; (B) $\epsilon_{sys}$ RVFW; (C) $SR_{sys}$ global RV; (D) $SR_{sys}$ RVFW; (E) $SR_e$ global RV; (F) $SR_e$ RVFW; (G) $SR_a$ global RV; and (H) $SR_a$ RVFW.**

Many of the recent efforts to assess RV function have used tissue velocity (Doppler) signals to assess velocity at the tricuspid annulus.[22,23] Researchers have demonstrated the ability of DTI to characterize global and regional myocardial motion, or deformation, with high temporal resolution, but the angle dependency of Doppler, high noise-to-signal ratio and interobserver variability is an unavoidable limitation.[21,28] Conversely, the alternative method for motion estimation proposed here is based on 2D feature tracking using VVI processing, a novel approach that is inherently 2D and independent of both cardiac translation and interrogation angle, as it tracks speckle patterns (acoustic markers) within serial B-mode sector scans.[21,29]

RV global function as estimated by $\epsilon_{sys}$ determines the total amount of local deformation of RV wall segments, while SR which reflects the rate of myocardial deformation, developed by estimating the spatial gradients in myocardial velocities.

VVI echocardiography represents a simplified and angle-independent modality for quantification of regional RV and LV myocardial deformation. Longitudinal strain and strain rate are more sensitive in assessment of subclinical systolic and diastolic dysfunction of the heart.[16,17] To the best of our knowledge, this is the first study to analyze RV regional deformation by the use of feature tracking VVI technology in patients affected by HCM.

### RV function in hypertrophic cardiomyopathy

The current AHA classification of cardiomyopathies defines HCM as a disease with left and/or right ventricular hypertrophy, which is usually asymmetric and involves the interventricular septum.[30,31]. Using cardiovascular MRI, Maron et al.[18] demonstrated that morphological RV abnormalities are present in a substantial fraction of patients with HCM. In the current study 49% of our patient population had increased RV wall thickness, and 21% had RV apical trabecular hypertrophy. In a recent report by Morner et al.[32] patients with HCM showed impaired global and regional RV tissue Doppler-derived myocardial performance index, with respect to healthy controls.

Similarly, the present study finds an RV and LV myocardial systolic and diastolic dysfunction at global and regional level using VVI and loss of base-to-apex gradient, despite normal LV ejection fraction and without evidence of clinical RV dysfunction.

Our results highlight a systolic asynchronicity involving the RV free wall and septum in HCM, the electromechanical delay between RV segments and prevalence of PSS and diminished RV myocardial deformation, which is not related to PAP, might be explained on the grounds of a direct involvement of RV wall by myopathic process.

On the other hand, the lower LV myocardial deformation indexes and its independent determination of RV dysfunction suggest ventricular interaction as further explanation of impairment in RV function in HCM. Ventricular interaction is an expression of close anatomic association between the two ventricles, which are encircled by common muscle fibres, share a septal wall, and are enclosed within the pericardium, and this is strengthened in our study by the close relation between deterioration of RV deformation and the magnitude of LV hypertrophy and aggressiveness of LV phenotype.

Interestingly, the present study cites the existence of extreme myocardial systolic non-uniformity and asynchrony in HCM, even in absence of intraventricular conduction delay. RV deformation was strongly related to intra-V asynchrony, which is the most powerful predictor of sudden cardiac death[21,22] and provided significant incremental prognostic value according to previous studies.[32,33] Such association between LV dyssynchrony and RV dysfunction could be part of a more critical phenotype and explain the increased risk of sudden cardiac death in HCM.

Additional longitudinal studies by 2D strain analyses are warranted to advance our understanding of the natural history of RV myocardial deformation in HCM, the extent of reversibility of RV dysfunction with medical therapy, and the possible long-term impact of such changes on patient outcomes.

## STUDY LIMITATION

Our study has several limitations. The first is that the feature tracking method is influenced by image quality; they can present limitations due to the physiological growth of the myocardial chambers, which prevents, sometimes, the perfect framing of the image in the echocardiographic window. The resolution of 2D imaging may be a problem in some subjects, and inadequate border recognition may be another factor limiting assessment of RV strain.

The second is that no analysis of gene mutation status was performed to offer further insight into genotype-phenotype relationships.

Finally, myocardial contractility is a complex mechanism; in the present study we investigated only the longitudinal deformation while the other components of wall deformation, like radial strain, circumferential are not included. However, approaching longitudinal myocardial function may be adequate, since 80% of total stroke volume is generated by longitudinal shortening. This better reflects myocardial function and may allow easier patient follow up in our daily practice.

## CONCLUSION

The impairment of RV myocardial deformation is evident in HCM using feature tracking. It is independently influenced by LV mechanics and correlated to the severity of LV phenotype. RV free-wall assessment of myocardial deformation and the results of RV global and regional involvement in HCM were comparable. Feature tracking, using this VVI approach, represents a promising and feasible non-invasive technique to provide more accurate analysis of regional function and uncover the subclinical RV involvement in HCM. The role of 2D strain imaging for stratifying the extent of myocardial abnormalities and future risk in HCM needs therefore further prospective evaluation.

## Acknowledgements

We greatly appreciate the assistance of: Sarah Moharem Elgamal (Assistant Specialist, National Heart Institute), Heba Kassem, (Assistant Professor, Pathology and Medical Genetics, Alexendria University), Ahmed El Guindy (Clinical Support Service, Aswan Heart Center) for their patient referrals and clinical consultation.

### REFERENCES

[1] Yacoub MH. Two hearts that beat as one. *Circulation*. 1995 Jul;92(2):156–157.
[2] Redington AN. Right ventricular function. *Cardiol Clin*. 2002 Aug;20(3):341–349, v. Review.
[3] Badano LP, Ginghina C, Easaw J, Muraru D, Grillo MT, Lancellotti P, Pinamonti B, Coghlan G, Marra MP, Popescu BA, De Vita S. Right ventricle in pulmonary arterial hypertension: haemodynamics, structural changes, imaging, and proposal of a study protocol aimed to assess remodeling and treatment effects. *Eur J Echocardiogr*. 2010;11:27–37.
[4] Maron BJ, Towbin JA, Thiene G, Antzelevitch C, Corrado D, Arnett D, Moss AJ, Seidman CE, Young JB, American Heart Association; Council on Clinical Cardiology, Heart Failure and Transplantation Committee; Quality of Care and Outcomes Research and Functional Genomics and Translational Biology Interdisciplinary Working Groups; Council on Epidemiology and Prevention. Contemporary definitions and classification of the cardiomyopathies. An American Heart Association Scientific Statement from the Council on Clinical Cardiology, Heart Failure and Transplantation Committee; Quality of Care and Outcomes Research and Functional Genomics and Translational Biology Interdisciplinary Working Groups; and Council on Epidemiology and Prevention. *Circulation*. 2006;113:1807–1816.
[5] Maron MS, Olivotto I, Betocchi S, Casey SA, Lesser JR, Losi MA, Cecchi F, Maron BJ. Effect of left ventricular outflow tract obstruction on clinical outcome in hypertrophic cardiomyopathy. *N Engl J Med*. 2003;348:295–303.
[6] Maron MS, Olivotto I, Zenovich AG, Link MS, Pandian NG, Kuvin JT, Nistri S, Cecchi F, Udelson JE, Maron BJ. Hypertrophic cardiomyopathy is predominantly a disease of left ventricular outflow tract obstruction. *Circulation*. 2006;114:2232–2239.
[7] Rigolin VH, Robiolio PA, Wilson JS, Harrison JK, Bashore TM. The forgotten chamber: the importance of the right ventricle. *Cathet Cardiovasc Diagn*. 1995;35:18–28.
[8] McLaughlin VV, Sitbon O, Badesch DB, Barst RJ, Black C, Galiè N, Rainisio M, Simonneau G, Rubin LJ. Survival with first-line bosentan in patients with primary pulmonary hypertension. *Eur Respir J*. 2005;25:244–249.
[9] Chin KM, Nick HS, Rubin LJ. The right ventricle in pulmonary hypertension. *Coron Art Dis*. 2005;16:13–18.
[10] Bristow MR, Zisman LS, Lowes BD, Abraham WT, Badesch DB, Groves BM, Voelkel NF, Lynch DM, Quaife RA. The pressure-overloaded right ventricle in pulmonary hypertension. *Chest*. 1998;114:101S–106S.
[11] Quaife RA, Chen MY, Lynch D, Badesch DB, Groves BM, Wolfel E, Robertson AD, Bristow MR, Voelkel NF. Importance of right ventricular end-systolic regional wall stress in idiopathic pulmonary hypertension: a new method for estimation of right ventricular wall stress. *Eur J Med Res*. 2006;11:214–220.
[12] Leuchte HH, Holzapfel M, Baumgartner RA, Ding I, Neurohr C, Vogeser M, Kolbe T, Schwaiblmair M, Behr J. Clinical significance of brain natriuretic peptide in primary pulmonary hypertension. *J Am Coll Cardiol*. 2004;43:764–770.
[13] Yang HS, Mookadam F, Warsame TA, Khandheria BK, Tajik JA, Chandrasekaran K. Evaluation of right ventricular global and regional function during stress echocardiography using novel velocity vector imaging. *Eur J Echocardiogr*. 2010;11(2):157–164.
[14] Korinek J, Kjaergaard J, Sengupta PP, Yoshifuku S, McMahon EM, Cha SS, Khandheria BK, Belohlavek M. High spatial resolution speckle tracking improves accuracy of 2-dimensional strain measurements: an update on a new method in functional echocardiography. *J Am Soc Echocardiogr*. 2007;20:165–170.
[15] Dalen H, Thorstensen A, Aase SA, Ingul CB, Torp H, Vatten LJ, Stoylen A. Segmental and global longitudinal strain and strain rate based on echocardiography of 1266 healthy individuals: the HUNT study in Norway. *Eur J Echocardiogr*. 2010 Mar;11(2):176–183.
[16] Vannan MA, Pedrizzetti G, Li P, Gurudevan S, Houle H, Main J, Jackson J, Nanda NC. Effect of cardiac resynchronization therapy on longitudinal and circumferential left ventricular mechanics by velocity vector imaging: description and initial clinical application of a novel method using high-frame rate B-mode echocardiographic images. *Echocardiography*. 2005;22(10):826–830.
[17] Bussadori C, Moreo A, Di Donato M, De Chiara B, Negura D, Dall'Aglio E, Lobiati E, Chessa M, Arcidiacono C, Dua JS, Mauri F, Carminati M. A new 2D-based method for myocardial velocity strain and strain rate quantification in a normal adult and paediatric population: assessment of reference values. *Cardiovasc Ultrasound*. 2009;13:7–8.
[18] Maron BJ, McKenna WJ, Danielson GK, Kappenberger LJ, Kuhn HJ, Seidman CE, Shah PM, Spencer WH III, Spirito P, Ten Cate FJ, Wigle ED, ACCF Task Force on Clinical Expert Consensus Documents Members; ESC Committee for Practice Guidelines Members. American College of Cardiology/European Society of Cardiology Clinical Expert Consensus Document on Hypertrophic Cardiomyopathy. A report of the American College of Cardiology Foundation Task Force on

Clinical Expert Consensus Documents and the European Society of Cardiology Committee for Practice Guidelines. *Eur Heart J*. 2003;24:1965–1991.
[19] Ishikawa T. Limitations and problems of assessment of mechanical dyssynchrony in determining cardiac resynchronization therapy indication. Is assessment of mechanical dyssynchrony necessary in determining CRT indication? (Con). *Circ J*. 2011 Feb;75(2):465–471. Epub Jan 8, 2011.
[20] Mele D, Pasanisi G, Capasso F, De Simone A, Morales MA, Poggio D, Capucci A, Tabacchi G, Sallusti L, Ferrari R. Left intra ventricular myocardial deformation dyssynchrony identifies responders to cardiac resynchronization therapy in patients with heart failure. *Eur Heart J*. 2006;27:1070–1078.
[21] D'Andrea A, Caso P, Cuomo S, Salerno G, Scarafile R, Mita C, De Corato G, Sarubbi B, Scherillo M, Calabrò R. Prognostic value of intra-left ventricular electromechanical asynchrony in patients with mild hypertrophic cardiomyopathy compared with power athletes. *Br J Sports Med*. 2006;40:244–250.
[22] D'Andrea A, Caso P, Sarubbi B, D'Alto M, Giovanna Russo M, Scherillo M, Cotrufo M, Calabrò R. Right ventricular myocardial activation delay in adult patients with right bundle branch block late after repair of Tetralogy of Fallot. *Eur J Echocardiogr*. 2004;5:123–131.
[23] Buckberg GD, RESTORE Group. The ventricular septum: the lion of right ventricular function, and its impact on right ventricular restoration. *Eur J Cardiothorac Surg*. 2006 Apr;29(Suppl 1):S272–S278. Epub Mar 29, 2006.
[24] Maeda M, Yamakado J, Nakano T. Right ventricular diastolic function in patients with hypertrophic cardiomyopathy. An invasive study. *Jpn Circ J*. 1999;63:681–687.
[25] Suzuki J, Chang JM, Caputo GR, Higgins CB. Evaluation of right ventricular early diastolic filling by cine nuclear magnetic resonance imaging in patients with hypertrophic cardiomiopathy. *J Am Coll Cardiol*. 1991;18:120–126.
[26] Okamoto M, Kinoshita N, Miyatake K, Nagata S, Beppu S, Park YD, Pyon ZF, Sakakibara H, Nimura Y. Diastolic filling of right ventricle in hypertrophic cardiomyopathy studied with 2-dimensional Doppler echocardiography. *J Cardiogr*. 1983;13:79–88.
[27] Lazzaret F, Pellerin D, Fournier C, Witchitz S, Veyrat C. Right and left isovolumic ventricular relaxation time intervals compared in patients by means of a singlepulsed Doppler method. *J Am Soc Echocardiogr*. 1997;10:699–706.
[28] D'Andrea A, De Corato G, Scarafile R, Romano S, Reigler L, Mita C, Allocca F, Limongelli G, Gigantino G, Liccardo B, Cuomo S, Tagliamonte G, Caso P, Calbrò R. Left atrial myocardial function in either physiological or pathological left ventricular hypertrophy: a two-dimensional speckle strain study. *Br J Sports Med*. 2008;42:696–702.
[29] Purushottam B, Parameswaran AC, Figueredo VM. Dyssynchrony in obese subjects without a history of cardiac disease using velocity vector imaging. *J Am Soc Echocardiogr*. 2011 Jan;24(1):98–106.
[30] Severino S, Caso P, Cicala S, Galderisi M, de Simone L, D'Andrea A, D'Errico A, Mininni N. Involvement of right ventricle in left ventricular hypertrophic cardiomyopathy: analysis by pulsed doppler tissue imaging. *Eur J Echocardiogr*. 2000;1:281–288.
[31] D'Andrea A, Caso P, Severino S, Sarubbi B, Forni A, Cice G, Esposito N, Scherillo M, Cotrufo M, Calabrò R. Different involvement of right ventricular myocardial function in either physiologic or pathologic left ventricular hypertrophy: a Doppler tissue study. *J Am Soc Echocardiogr*. 2003;16:154–161.
[32] Morner S, Lindqvist P, Waldenstrom A, Kazzam E. Right ventricular dysfunction in hypertrophic cardiomyopathy as evidenced by the myocardial performance index. *Int J Cardiol*. 2008;124:57–63.
[33] D'Andrea A, Caso P, Severino S, Scotto di Uccio F, Vigorito F, Ascione L, Scherillo M, Calabrò R. Association between intraventricular myocardial systolic dyssynchrony and ventricular arrhythmias in patients with hypertrophic cardiomyopathy. *Echocardiography*. 2005;22:571–578.